Carbohydrate Polymers 96 (2013) 21–30

Contents lists available at SciVerse ScienceDirect

Carbohydrate Polymers

journal homepage: www.elsevier.com/locate/carbpol

Ultrasound-assisted formation of the canthaxanthin emulsions stabilized by arabic and xanthan gums

Seyed Mohammad Taghi Gharibzahedi, Seyed Hadi Razavi*, Seyed Mohammad Mousavi

Bioprocess Engineering Laboratory (BPEL), Department of Food Science, Engineering and Technology, Faculty of Agricultural Engineering and Technology, University of Tehran, P.O. Box 4111, Karaj 31587-77871, Iran

ARTICLE INFO

Article history:
Received 21 February 2013
Received in revised form 11 March 2013
Accepted 26 March 2013
Available online 2 April 2013

Keywords:
Canthaxanthin emulsion
Emulsion stability
Particle size
Entrapment efficiency
Ultrasound
Response surface optimization

ABSTRACT

There is interest in incorporating canthaxanthin (CTX) into food emulsions due to its high potential health benefits. The used CTX in this study was produced by the bacterium of *Dietzia natronolimnaea* HS-1. Then, the influence of main emulsion components (gum arabic (GA), xanthan gum (XG) and coconut oil (CO)) on the surface-weighted mean diameter (D_{32}), polydispersity index (PDI), specific surface area (SSA) of droplets and density of the emulsions containing CTX was optimized using response surface methodology (RSM). Polynomial equations between the responses and independent variables were derived. The linear effect of GA had a significant ($p < 0.0001$) term in all reduced models. The optimal formulation for emulsions was composed of GA content of 9.85% (w/w), XG content of 0.13% (w/w) and CO concentration of 3.50% (w/w). This optimum formulation yielded D_{32} of 0.752 μm, PDI of 1.533, SSA of 9.995 m^2/ml and density of 1.0357 g/cm^3.

1. Introduction

Oil-in-water (O/W) emulsions are considered to be very important fluids due to their specific properties and applications in medicine and the petroleum, chemical, and food industries (Huang, Kakuda, & Cui, 2001; Rousseau, 2000). Since the contact between oil and water molecules is energetically unfavorable, emulsions are thermodynamically unstable systems (Harnsilawat, Pongsawatmanit, & Mcclements, 2006). Emulsion stability is characterized in various mechanisms – creaming or sedimentation, flocculation of droplets, coalescence between droplets, or phase separation (Gharibzahedi, Mousavi, Hamedi, & Ghasemlou, 2012; Granato, Castro, Neves, & Masson, 2010). Stoke's law explains that the velocity at which a droplet moves is inversely proportional to the viscosity of water phase and directly proportional to the square of the droplet size radius and density difference between water and oil phases (Taherian, Fustier, & Ramaswamy, 2006). Therefore, reducing droplet size along with increasing density of oil droplet and viscosity of water phase can enhance the emulsion stability (Chanamai & McClements, 2000).

Hydrocolloids are used as stabilizers and emulsifiers in O/W emulsions. Most hydrocolloids can act as stabilizers (stabilizing agents) of the emulsions, but only a few can act as emulsifiers (emulsifying agents) (Harnsilawat et al., 2006). A suitable hydrocolloid for the concentrated emulsions need to have high emulsifying capacity, high solubility in cold water, low viscosity in solution, and no gelling and/or thickening effects for a special period of time (Dickinson, Galazka, & Anderson, 1991). It is well documented that gum arabic (GA), a natural polysaccharide, has excellent emulsification properties for some emulsions (Buffo, Reineccius, & Oehlert, 2001; Dłuzewska, Stobiecka, & Maszewska, 2006; Gharibzahedi, Mousavi, Hamedi, & Ghasemlou, 2012; Gharibzahedi, Mousavi, Hamedi, Khodaiyan, Razavi, 2012; Gharibzahedi, Mousavi, Khodaiyan, & Hamedi, 2012; Tan, 1990). This hydrocolloid is surface active, adsorbs to interfaces between oil and water, and facilitates the production of small droplets by lowering the interfacial tension during homogenization (Buffo et al., 2001). Xanthan gum (XG) is an anionic heteropolysaccharide produced by the bacterium, *Xanthomonas campestris* and has a particularly complicated molecular structure (Higiro, Herald, & Alavi, 2006). It has been extensively applied due to its excellent viscosity and dispersion (e.g. the reversible shear-thinning, dispersed in either hot or cold water) characteristics. Therefore, this biopolymer tends to form in solution structures, showing high low-shear and weak gel properties that lend stability to colloidal suspensions (Nikiforidis & Kiosseoglou, 2010). Gharibzahedi, Mousavi, Hamedi, Khodaiyan, et al. (2012) and Gharibzahedi, Mousavi, Hamedi, & Khodaiyan (2013) showed that the use of GA biopolymer in combination with XG can increase physicochemical stability of walnut oil-in-water emulsions.

* Corresponding author. Tel.: +98 26 3224 8804; fax: +98 26 3224 9453.
E-mail address: srazavi@ut.ac.ir (S.H. Razavi).

0144-8617/$ – see front matter © 2013 Elsevier Ltd. All rights reserved.
http://dx.doi.org/10.1016/j.carbpol.2013.03.085

Functional foods are made up of natural components that impart nutritional benefits to human health. Carotenoids are examples of these components which, in addition to their inherent nutritional value, also contribute to the taste and colour of foods (Batista, Raymundo, Sousa, & Empis, 2006). Among the produced carotenoids, β-carotene and the xanthophylls astaxanthin, canthaxanthin (CTX), and lutein are the major compounds with particular commercial interest (Hojjati, Razavi, Rezaei, & Gilani, 2011). CTX (4,4′-diketo-β-carotene) is an orange-red ketocarotenoid with high antioxidant activity. Production of this pigment from biological resources with regarding to restriction of synthetic carotenoids in different industries has recently developed throughout in the world (Gharibzahedi, Razavi, & Mousavi, 2012; Gharibzahedi, Razavi, & Mousavi, Moayedi, 2012). Among the introduced sources, the bacterium of *Dietzia natronolimnaea* HS-1 is recognized as a promising producer of natural CTX (Khodaiyan, Razavi, & Mousavi, 2008). Therefore, the emulsions enrichment with CTX produced by *D. natronolimnaea* HS-1 can increase consumer's demand for consumption of these products.

Response surface methodology (RSM) is a useful statistical procedure used for multiple regression analysis by using quantitative data. This technique solves multivariate data which is found from appropriately designed experiments to solve multivariate equation simultaneously (Baş & Boyaci, 2007). Moreover, the main advantage of RSM is to reduce number of experimental trials needed to evaluate multiple variables and their interactions. Therefore, RSM is less laborious and time-consuming than the classical methods required optimizing a process (Cruz, Faria, Granato, Cavalcanti, & Walter, 2010; Myers & Montgomery, 2002).

The aim of this work was to optimize the droplet size and density properties of coconut oil (CO)-in-water emulsions containing bacterial CTX using RSM. In the present study, RSM was used. The optimization of emulsion components (GA, XG and CO) levels allows the manufacturers for the pre-formulation of optimum CTX emulsions with desirable physical characteristics.

2. Materials and methods

2.1. Chemicals and materials

Potassium sorbate was obtained from Chisso Co. (Tokyo, Japan). Sodium benzoate was provided by Fars Chemical Industry Co. (Shiraz, Iran) and food grade citric acid (anhydrous) was purchased from Kimia Gharb-Gostar Industry Co. (Kermanshah, Iran). GA was purchased from Merck KGaA (Darmstadt, Germany). XG was provided from Sigma–Aldrich (Oakville, ON, Canada). CO was purchased from local market. It was selected for emulsion production due to high saturated fatty acids and followed by reduction of oxidation problems. The used CO contained the following fatty acids (mol%): 7.9% C8:0, 6.5% C10:0, 45.6% C12:0, 18.3% C14:0, 8.7% C16:0, 2.9% C18:0, 7.1% C18:1 and 1.4% C18:2 as measured by gas chromatography of methyl esters.

2.2. Canthaxanthin extraction and analysis

The strain of bacterium *D. natronolimnaea* HS-1 (DSM 44860) used in this work to produce CTX was provided by Bioprocess Engineering Laboratory (BPEL), University of Tehran, Iran. Pigment extraction and analysis were performed as previously reported by Gharibzahedi, Razavi, & Mousavi (2013). Briefly, after preparing pre-culture in liquid yeast/malt agar medium, the inoculum was transferred into Erlenmeyer flasks containing 25 g/l beet root molasses and 10 g/l yeast extract. Finally, the flasks to produce CTX were incubated at 180 rpm and 28 ± 2 °C for 6 days. Then, aliquots (10-ml) of cultures were taken from the bioreactor and centrifuged at 7500 × *g* for 7.5 min. The produced supernatant was collected. Then, the cell pellets were washed twice with physiological water (NaCl; 9 g/l in deionized water) and centrifuged again. These cells were resuspended three times in 3 ml of pure ethanol by vortexing for 5 min and centrifuged again to extract the pigment. A water bath (45 °C) was also used to completely extract the pigments. The carotenoid extracts subsequently filtered through a 0.2 μm hydrophobic fluorophore membrane (Sigma–Aldrich Co., USA). Individual carotenoids were analyzed according to the modified method of Razavi, Blanchard, & Marc (2006) using a Knauer (Berlin, Germany) HPLC system on a Lichrospher 100 RP-18 silica column (5.0 mm, 250 mm × 4 mm) at 35 °C.

2.3. Preparation of emulsion samples

The emulsions were prepared according to the following formula: GA (6–10%, w/w), XG (0.1–0.3%, w/w), CO (3.5–6.5%, w/w), citric acid (0.4%, w/w), potassium sorbate (0.1%, w/w), sodium benzoate (0.1%, w/w) and deionized water. CTX was also added to CO fraction. Because of CTX negligible solubility at room temperature, it is dissolved in hot CO at a constant ratio of 1:50 to add it to the O/W emulsions. According to the previous study (Gharibzahedi, Razavi, et al., 2013), this ratio was an optimum level for the high solubility of CTX in CO

CTX is highly susceptible to thermal degradation, for that, the exposure time at high temperatures should be restricted. Authors previously examined various times and temperatures under vacuum conditions for achieving the lowest oxidation rate. The results showed that temperature of 97 °C and time 7.5 s at vacuum can lead to CTX high solubility with ideal oxidation level (Gharibzahedi, Razavi, & Mousavi, 2012). The peroxide value, anisidine value and total oxidation (Totox) value under these conditions were 0.22 mequiv. O_2/kg oil, 0.26 and 0.70, respectively. The main emulsion components (GA, XG and CO) were prepared for the optimization procedure based on a three-factor central composite design (CCD) (Table 1).

All emulsions containing microbial CX were prepared in two stages. The coarse emulsions were produced by Ultra Turrax (IKA T25 Digital, Germany) in 6000 × *g* for 10 min, and then further emulsified by using an 25 kHz ultrasonic homogeniser (UP200S, Hielscher Ultrasonics GmbH, Teltow, Germany) equipped with a 13-mm-diameter sonotrode probe made of titanium at a total nominal output power of 200 W. To prepare the water phase, citric acid, potassium sorbate and sodium benzoate were dispersed in deionised water (≈60 °C) using a blender (IKA-WERK, RW 20 DZM, Staufen, Germany). During continuous mixing, GA was gradually added to the deionized water (≈60 °C), and the solution was mixed for an extra 5 min to further facilitate hydration. To achieve full hydration, the mixture was kept at room temperature (23 ± 1 °C) overnight. XG solution was prepared separately by dissolving XG in deionized water with shaking and then mixed with the GA solution by using a high-speed blender (Gharibzahedi, Mousavi, et al., 2013). The dispersion of CTX in CO was also maintained overnight to rehydrate and then slowly added to the water phase to prepare an initial coarse emulsion. In the next stage, in order to produce the fine-disperse emulsions with small average droplet size and narrow particle-size distribution, the coarse emulsions were sonicated for 4 min (Gharibzahedi, Razavi, et al., 2013). By holding the vessel in a refrigerated water bath, the difference of temperature from initial coarse emulsions to final emulsion during emulsification was not more than 20 °C. At least two separate emulsions were prepared for each treatment. The emulsions were stored at 4 °C, and re-equilibrated to room temperature just before analysis.

Table 1
Experimental design matrix for CCRD-RSM and actual responses.

Point type	Run no.	Block	Independent variables			Response variables			
			X_1 [a]	X_2 [b]	X_3 [c]	D_{32} (Y_1, μm)[d]	PDI (Y_2)[e]	SSA (Y_3, m^2/ml)[f]	Density (Y_4, g/cm^3)
Fact	1	1	−1	−1	−1	0.963 ± 0.032	2.106 ± 0.035	7.95 ± 0.21	1.0194 ± 0.0003
Fact	2	2	1	−1	−1	0.738 ± 0.006	1.419 ± 0.0010	10.65 ± 0.13	1.0371 ± 0.0006
Fact	3	2	−1	1	−1	1.046 ± 0.002	2.051 ± 0.057	6.75 ± 0.06	1.0127 ± 0.0004
Fact	4	1	1	1	−1	0.633 ± 0.031	1.614 ± 0.062	8.52 ± 0.03	1.0185 ± 0.0005
Fact	5	2	−1	−1	1	0.811 ± 0.025	4.218 ± 0.051	5.70 ± 0.11	1.0116 ± 0.0001
Fact	6	1	1	−1	1	0.974 ± 0.027	2.583 ± 0.059	6.32 ± 0.16	1.0301 ± 0.0000
Fact	7	1	−1	1	1	0.948 ± 0.001	3.253 ± 0.002	6.80 ± 0.12	1.0132 ± 0.0009
Fact	8	2	1	1	1	0.964 ± 0.002	1.594 ± 0.056	9.31 ± 0.10	1.0259 ± 0.0006
Center	9	1	0	0	0	0.914 ± 0.040	2.574 ± 0.022	6.79 ± 0.65	1.0220 ± 0.0009
Center	10	1	0	0	0	0.901 ± 0.001	2.518 ± 0.082	6.16 ± 0.31	1.0212 ± 0.0001
Center	11	2	0	0	0	0.926 ± 0.002	2.641 ± 0.091	7.84 ± 0.01	1.0225 ± 0.0001
Center	12	2	0	0	0	0.918 ± 0.004	2.522 ± 0.043	7.55 ± 0.08	1.0222 ± 0.0001
Axial	13	3	−1.68	0	0	1.188 ± 0.035	4.081 ± 0.010	4.32 ± 0.09	1.0152 ± 0.0002
Axial	14	3	1.68	0	0	0.901 ± 0.002	1.912 ± 0.011	7.91 ± 0.05	1.0379 ± 0.0000
Axial	15	3	0	−1.68	0	0.822 ± 0.037	2.849 ± 0.009	7.02 ± 0.00	1.0234 ± 0.0008
Axial	16	3	0	1.68	0	0.742 ± 0.040	2.054 ± 0.018	7.48 ± 0.01	1.0155 ± 0.0009
Axial	17	3	0	0	−1.68	0.895 ± 0.006	1.692 ± 0.032	7.91 ± 0.09	1.0189 ± 0.0002
Axial	18	3	0	0	1.68	1.005 ± 0.001	3.467 ± 0.040	5.29 ± 0.04	1.0174 ± 0.0005
Center	19	3	0	0	0	0.945 ± 0.010	2.880 ± 0.008	6.51 ± 0.42	1.0215 ± 0.0002
Center	20	3	0	0	0	0.978 ± 0.022	2.932 ± 0.045	5.98 ± 0.23	1.0208 ± 0.0009

[a] The five levels (−1.682, −1, 0, +1 and +1.682) of factor X_1 (gum arabic (GA) content) represented 4.64, 6.00, 8.00, 10.00 and 11.36% (w/w), respectively.
[b] The five levels (−1.682, −1, 0, +1 and +1.682) of X_2 (xanthan gum (XG) content) represented 0.03, 0.10, 0.20, 0.30 and 0.37% (w/w), respectively.
[c] The five levels (−1.682, −1, 0, +1 and +1.682) of X_3 (coconut oil (CO) content) represented 2.48, 3.50, 5.00 6.50 and 7.52% (w/w), respectively.
[d] Surface-weighted mean diameter.
[e] Polydispersity index.
[f] specific surface area of droplets.

2.4. Droplet size measurement

Average droplet size of the emulsions was measured using a Malvern Mastersizer 2000 laser diffraction particle size analyzer (Malvern Instruments Ltd., Worcestershire, UK). Sample analysis was carried out after the emulsions were stored for 24 h at room temperature, based on Mie theory (Huang et al., 2001). The concentrated emulsions were diluted with deionized water (1:100) to avoid multiple scattering effects, and placed directly into a metal jar that circulated the sample through the measuring-glass cuvette. A laser beam directed through the diluted emulsions was scattered by the droplets in a characteristic pattern according to their size and detected by an array of photodiodes located behind the cuvette. Size distribution was characterized by volumetric percentage and mean droplet diameter obtained by surface-weighted mean diameter (D_{32}) of the emulsion droplets, based on the following Eq. (1) (Gharibzahedi, Mousavi, Khodaiyan, & Hamedi, 2012):

$$D_{32} = \frac{\sum n_i d_i^3}{\sum n_i d_i^2} \quad (1)$$

where n_i is the number of droplets of diameter d_i.

The distribution width of droplets size known as polydispersity index (PDI) was determined from the following Eq. (2) (Koocheki & Kadkhodaee, 2011):

$$\mathrm{PDI} = \frac{[d(\upsilon, 90) - d(\upsilon, 10)]}{d(\upsilon, 50)} \quad (2)$$

where $d(\upsilon, 10)$, $d(\upsilon, 50)$, and $d(\upsilon, 90)$ are diameters at 10%, 50%, and 90% cumulative volume, respectively. In other words, $[d(\upsilon, 90) - d(\upsilon, 10)]$ is the range of the data and $d(\upsilon, 0.5)$ is the median diameter. Therefore, a smaller PDI value indicates a more uniform in the droplet size.

The specific surface area (SSA) based on the method described by Gharibzahedi, Mousavi, Khodaiyan, et al. (2012) was calculated according to the Eq. (3):

$$\mathrm{SSA} = \frac{6\phi}{D_{32}} (\mathrm{m^2/ml\ \ emulsion}) \quad (3)$$

where ϕ represents the oil volume fraction of the emulsion.

2.5. Density measurement

The density of emulsions was determined in triplicate at room temperature by a digital densitometer (AP-PAAR DMA 46, Germany) with an accuracy of 10^{-4} g/cm^3. The mean of measurement values found was taken as a response value for fitting the model and data analysis.

2.6. Emulsion stability

Stability of the optimum emulsions was evaluated by measuring the extent of gravitational phase separation. For the measurement of physical stability, freshly prepared emulsions (15 ml) were transferred into cylindrical glass tubes (internal diameter 10 mm, height 120 mm), capped and stored for 30 days at room temperature. The emulsion stability index (ESI) was calculated as follows (Eq. (4)):

$$\mathrm{ESI}(\%) = \left(\frac{H_E - (H_C + H_S)}{H_E}\right) \times 100\% \quad (4)$$

where H_E is percentage of the initial emulsion height, H_S is the height of the sedimentation phase and H_C is the height of the cream layer.

2.7. Determination of CTX entrapment efficiency

The CTX entrapment efficiency of the optimum emulsions was evaluated as described by Yue et al. (2009). Briefly, in a Beckman L8-M Ultracentrifuge (Beckman Instruments Inc., USA), about 3 ml of the emulsion was ultracentrifuged at 162,000 × g at 4 °C for 1 h. The

entrapment efficiency (EE) of CTX was determined by measuring the amount of CTX (C_W) in the water layer obtained after ultracentrifugation (UC). The EE was determined using Eq. (5) given below:

$$EE\% = \left(1 - \frac{C_W}{C_T} \times r\right) \times 100\% \quad (5)$$

where C_T is the concentration of CTX and r is the ratio of the aqueous phase volume of the emulsion to the total volume.

2.8. Experimental design and optimization method

The content of main emulsion components were optimized by RSM. A central composite rotatable design (CCRD) was used in this regard. The effect of GA content (X_1), XG content (X_2) and CO concentration (X_3) as three independent variables on D_{32} (Y_1), PDI (Y_2), SSA (Y_3) and density (Y_4) of CTX emulsions was evaluated.

Preliminary experiments were carried out to determine the effect of various operating conditions in the ultrasonic emulsification (applied power, ultrasound frequency and process time) on the particle size and also the best preparation conditions to obtain a small mean particle size (0.759 ± 0.102 μm) and narrow size distribution. The results revealed that fine emulsification by ultrasonic treatment obtained at applied power 200 W, frequency 25 kH and running time 115 s (data not shown). After preliminary tests, the range and centre point values of three independent factors were studied at 5 levels (± 1.682, ± 1 and 0) and 20 experiments was carried out randomly (Table 1). The experimental design consists of eight factorial points, six axial points at a distance of ± 1.682 from the center and six replicates of the central point (Table 1).

For the statistical treatment, the actual factors were coded according to this equation:

$$x = \frac{X_i - X_0}{\Delta X}, \quad i = 1, 2, 3 \quad (6)$$

where x is the coded value of the variable, X_i is the actual value of the variable, X_0 is the actual value of X_i on the central point, and ΔX is the step-change value. The results of the experimental design were fitted with a second-order polynomial equation by a multiple regression technique. The quadratic equation to predict the optimal point was explained as follows:

$$Y = a_0 + \sum_{i=1}^{3} a_i X_i + \sum_{i=1}^{3} a_{ii} X_i^2 + \sum_{i=1}^{2} \sum_{j=1+1}^{3} a_{ij} X_i X_j + \varepsilon \quad (7)$$

where Y is the dependent variables (D_{32}, PDI, SSA and density), a_0 is the model constant, a_i, a_{ii} and a_{ij} are the model coefficients, and ε is the error. They represent the linear, quadratic and interaction effects of the variables.

The quality of the fit of polynomial model was statistically checked by means of the coefficient of determination (R^2), adjusted R^2 (R^2_{adj}), the predicted error sum of squares (PRESS), the root mean square error of prediction (RMSEP), the relative standard error of prediction (RSEP) and absolute average deviation (AAD) (Gharibzahedi, Razavi, Mousavi, & Moayedi, 2012).

The PRESS statistic is calculated as Eq. (8) (Baş & Boyaci, 2007):

$$PREES = \sqrt{\sum_{i=1}^{N} (y_{pre,i} - y_{exp,i})^2} \quad (8)$$

In other words, for calculating this parameter, each observation is omitted in turn whereas the remaining sites are used to fit the model. This new regression model is applied to predict the withheld observation and its resulting residual or error. The PRESS parameter is described as the sum of squares of the PRESS residuals and can be employed in place of the sum of square residuals to calculate an R^2 for prediction (Myers & Montgomery, 2002):

$$R^2_{prediction} = 1 - \frac{PREES}{SS_T} \quad (9)$$

Table 2
Regression coefficients and evaluation of mathematical models for the response variables.

Regression coefficient	Response variables			
	D_{32} (Y_1, μm)[a]	PDI (Y_2)[b]	SSA (Y_3, m^2/ml)[c]	Density (Y_4, g/cm^3)
a_0	0.930	2.68	6.80	1.0217
a_1	−0.06	−0.59	1.00	0.0068
a_2	–	−0.23	–	−0.0030
a_3	0.03	0.55	−0.74	−0.0007
a_1^2	0.03	–	–	0.0016
a_2^2	−0.06	−0.15	0.41	−0.0008
a_3^2	–	−0.11	0.18	−0.0013
$a_1\ a_2$	−0.04	–	–	−0.0022
$a_1\ a_3$	0.10	−0.27	–	0.0009
$a_2\ a_3$	–	−0.26	0.93	0.0028
Regression (p-value)	<0.0001[d]	<0.0001[d]	<0.0001[d]	<0.0001[d]
Lack-of-fit (p-value)	0.074[e]	0.251[e]	0.794[e]	0.078[e]
Residual	0.007	0.05	0.67	0.000
Pure error	0.0006	0.01	0.38	0.000
Total	0.274	11.72	38.78	0.0009
R^2	0.970	0.995	0.979	0.992
R^2_{adj}	0.936	0.990	0.955	0.984
$R^2_{prediction}$	0.912	0.928	0.901	0.931
CV	3.47	3.10	4.05	0.09
PRESS	0.089	0.223	0.805	0.002
RMSEP	0.019	0.049	0.180	0.0005
RSEP	2.169	1.875	2.518	0.058
AAD	1.838	1.733	2.017	0.047
Adequate precision	22.64	46.60	28.11	36.25

[a] Surface-weighted mean diameter.
[b] Polydispersity index.
[c] Specific surface area of droplets.
[d] Significant ($p < 0.0001$)
[e] Not significant ($p > 0.05$).

Table 3
The significance of each response variable effect showed by using *F*-ratio and *p*-value in the nonlinear reduced order models.

Response variables	D_{32} (Y_1, μm)[a]		PDI (Y_2) [b]		SSA (Y_3, m^2/ml) [c]		Density (Y_4, g/cm^3)	
	p-value	*F*-ratio	*p*-value	*F*-ratio	*p*-value	*F*-ratio	*p*-value	*F*-ratio
Linear effects								
X_1 (GA)	<0.0001*	64.99	<0.0001*	763.45	<0.0001*	162.92	<0.0001*	711.18
X_2 (XG)	0.8067	0.064	<0.0001*	116.52	0.1891	2.06	<0.0001*	139.85
X_3 (CO)	0.0026*	18.47	<0.0001*	650.13	<0.0001*	90.18	0.0268*	7.32
Quadratic effects								
X_1^2	0.0057*	13.97	0.0922	3.66	0.9475	0.0046	0.0002*	44.22
X_2^2	<0.0001*	54.82	<0.0001*	53.94	0.0007*	28.46	0.0086*	11.96
X_3^2	0.7917	0.075	0.0009*	26.73	0.0490*	5.38	0.0007*	28.18
Interaction effects								
X_1X_2	0.0056*	14.04	0.3414	1.02	0.2742	1.38	0.0002*	44.09
X_1X_3	<0.0001*	83.51	<0.0001*	94.33	0.1399	2.69	0.0202*	8.34
X_2X_3	0.1341	2.78	<0.0001*	87.84	<0.0001*	82.33	<0.0001*	72.52

[a] Surface-weighted mean diameter.
[b] Polydispersity index.
[c] Specific surface area of droplets.
* Significant at $p < 0.05$.

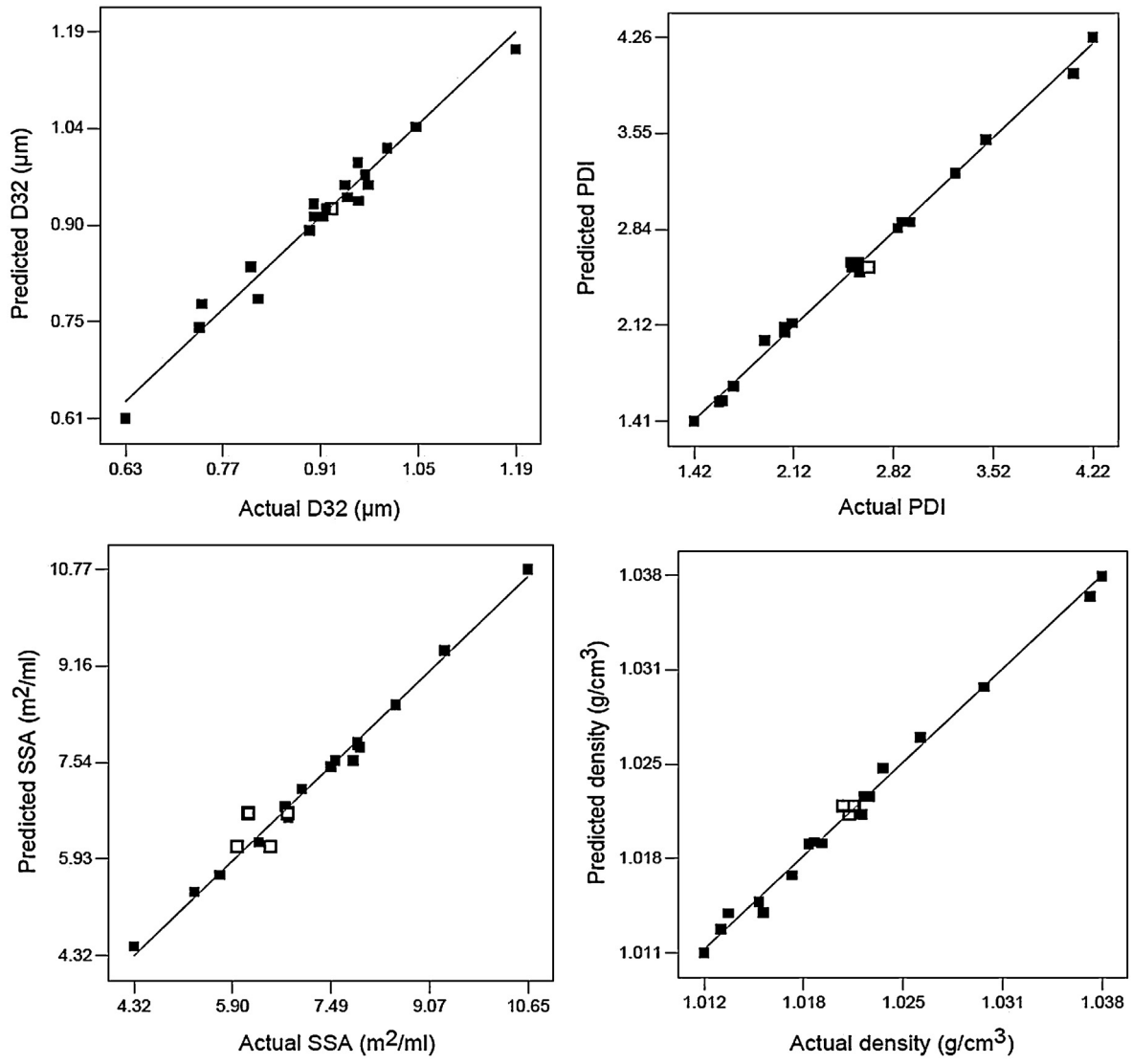

Fig. 1. Comparison between predicted and actual values of D_{32}, PDI, SSA and density of the emulsions containing bacterial CTX.

In Eqs. (8) and (9), $y_{i,exp}$ is the experimental responses, $y_{i,pre}$ is the predicted responses and SS_T is the total sum of the squares.

Adequate precision (AP) compares the range of the predicted values at the design points to the average prediction error. The definition of adequate precision is in Eqs. (10) and (11):

$$AP = \frac{\max(\bar{y}) - \min(\bar{y})}{\sqrt{\bar{V}(\bar{y})}} \quad (10)$$

where

$$\bar{V}(\bar{y}) = \frac{1}{N}\sum_{i=1}^{N} V(\bar{y}) = \frac{p\sigma^2}{N} \quad (11)$$

In Eqs. (10) and (11), $\bar{y}$ is the predicted value, p is the number of model parameters, σ^2 is the residual mean square from analysis of variance (ANOVA) table, and N is the number of experiments.

According to the ANOVA, the regression coefficients of individual linear, quadratic and interaction terms were determined. In order to visualize the relationship between the response and experimental levels of each factor and to deduce the optimum conditions, the regression coefficients were then used to make statistical calculation to generate three-dimensional (3-D) surface plots by changing two of all the variables within the experimental range while holding the other variables as constant values. The optimum region was also identified using the overlay plot. Design Expert (trial version 7.1.6, Stat-Ease Inc., Minneapolis, USA) statistical package was used for the experimental design and regression analysis of the experimental data. The statistical significance test was based on the total error criteria with confidence level of 95.0%.

3. Results and discussion

3.1. Fitting the response surface models

The determined regression coefficients of the models for the response variables, along with the corresponding p-value of lack of fit, R^2, adj-R^2, PRESS, RMSEP and AAD are given in Table 2. Each response variable was evaluated as a function of linear, quadratic and interaction effects of GA (X_1), XG (X_2) and CO (X_3). The individual significance F-value and p-value of independent variables including D_{32}, PDI, SSA and density of the emulsions containing CTX biosynthesized by *D. natronolimnaea* HS-1 are illustrated in Table 3. Multiple linear regression analysis of the experimental data yielded quadratic models for predicting the independent variables as postulated at the beginning of the research. The results of analysis of variance (ANOVA) indicate that the contribution of the quadratic models was very significant ($p < 0.0001$). Since the models have shown lack of fit to be insignificant the responses surfaces

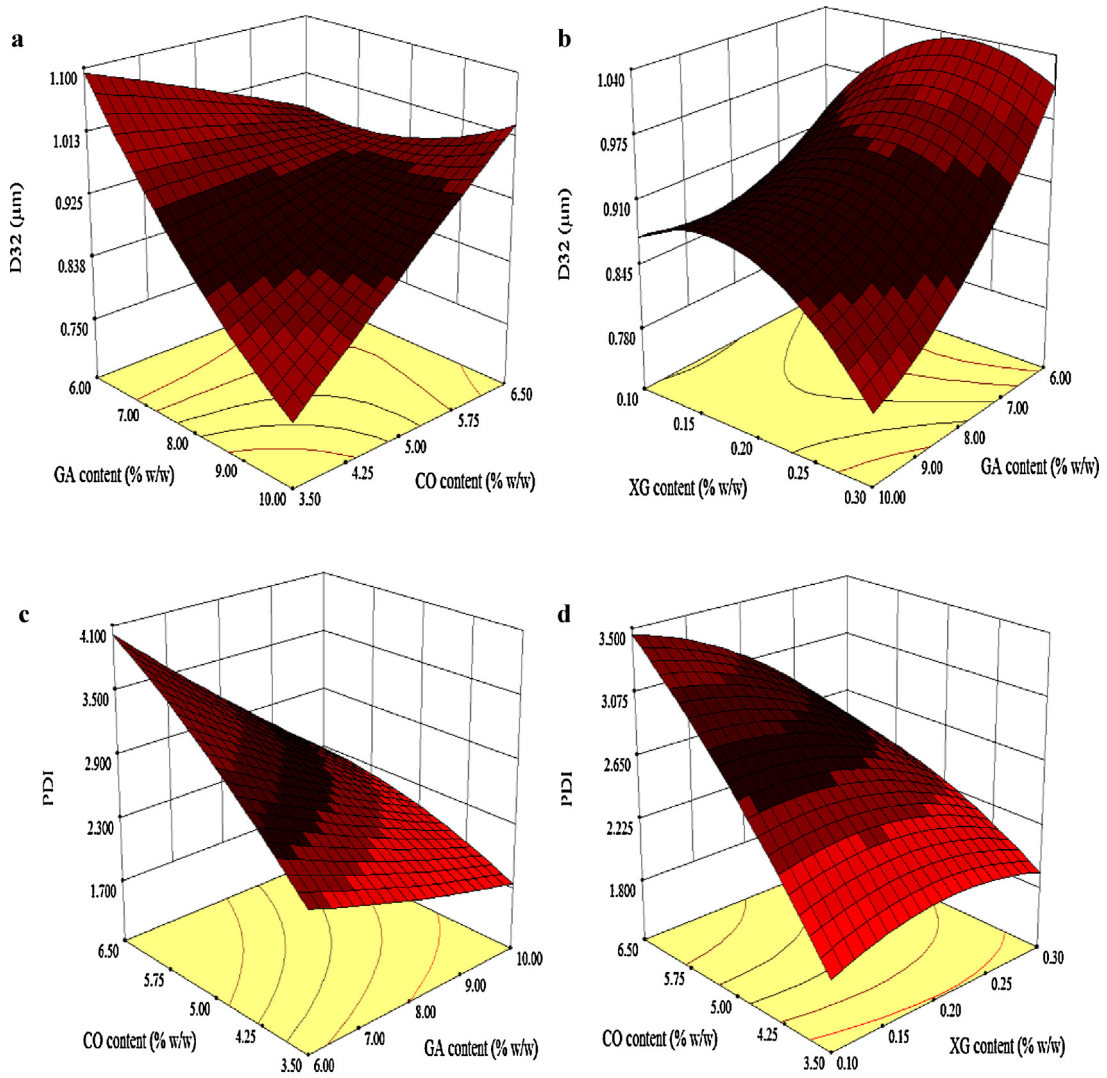

Fig. 2. 3D surface plots showing the significant ($p < 0.05$) interaction effects on the variation of D_{32} (a, b) and PDI (c, d) of the emulsions containing bacterial CTX.

(Table 2) were sufficiently explained by the regression equations. As exhibited in Table 2, the significant response surface models with high R^2, R^2_{adj} and $R^2_{prediction}$ values varied from 0.970 to 0.995, 0.936 to 0.990 and 0.901 to 0.931, respectively (Table 2). These values indicate adequacy of the applied models. Fig. 1 also reveals the comparison between the actual response values obtained from experimental data and the predicted response values based on the polynomial regression models and proves that the models cover the experimental range of studies sufficiently.

Moreover, the values of coefficient of variation (CV) were 3.47, 3.10, 4.05 and 0.09 for D_{32}, PDI, SSA and density, respectively. CV represents repeatability within the same treatments or reproducibility within different treatments (Myers & Montgomery, 2002). The RMSEP and RSEP values are used to evaluate the predictive ability of the selected models (Baş & Boyaci, 2007). A low PRESS (0.002–0.805), RMSEP (0.002–0.330) and RSEP (0.058–2.518) values suggest for the adequacy of the fitted quadratic models for predictive applications. The AAD values of the models were determined as 1.88, 1.73, 2.01 and 0.04 for D_{32}, PDI, SSA and density models, respectively (Table 2). Compared to the AAD values, Baş and Boyaci (2007) had reported for various experiments, AAD values for the models in this study were very reasonable. AP is a signal-to-noise ratio: it compares the range of predicted values at fixed levels to average prediction error. A ratio greater than 4 is desirable and indicates an adequate signal (Myers & Montgomery, 2002). It was found to be 22.64, 46.60, 28.11 and 36.25 for the D_{32}, PDI, SSA and density, respectively.

3.2. Analysis of influence of variables on surface-weighted mean diameter (D_{32})

The results indicated that the linear effects of GA and CO were significant ($p < 0.0001$, $p < 0.01$) on the D_{32} (Y_1); whereas XG is not significant (Table 3). Quadratic effect of GA concentration and XG content was significant at the 1% and 0.01% level, respectively. Also, the mutual interaction between GA concentration and XG content, and GA concentration and CO content were found to be significant ($p < 0.01$, $p < 0.0001$). The most significant ($p < 0.05$) effect on D_{32} was shown to be the interaction effect of GA and CO followed by the linear effect of GA and quadratic effect of XG (Table 2). As shown in Fig. 2a and b, the variation D_{32} of CTX emulsions could be explained as a nonlinear function of the main emulsion components. Increases in GA content resulted in reduced D_{32}, although this parameter increased sharply with increased CO concentration (Fig. 2a). The negative effect of GA on the D_{32} could be due to its surface activity and ability to form a protective film around emulsion droplets. In other words, the additional GA was able to coat the surface area and resulted in the formation of greater number of smaller droplets (Huang et al., 2001; Koocheki & Kadkhodaee, 2011). It was found that a CTX emulsion containing 9.85% (w/w) GA, 0.15% (w/w) XG and 3.50% (w/w) CO was predicted to result in the minimum D_{32} ($Y_1 = 0.633$ μm).

3.3. Analysis of influence of variables on polydispersity index (PDI) of droplets

As clearly exhibited in Table 3, all independent variable effects except for the quadratic effect of GA and its interaction with XG were found to be significant ($p < 0.0001$, $p < 0.001$) on the variation of PDI (Y_2). Fig. 2c reveals that at low CO concentration, increasing the GA content decreased the PDI, whereas at higher CO content, GA content had greater effect. Moreover, at low XG content, increasing CO content increased the PDI (Fig. 2d). The most significant effect on PDI was shown to be the main effect of GA followed by the main effect of CO and interaction effect of GA and CO contents.

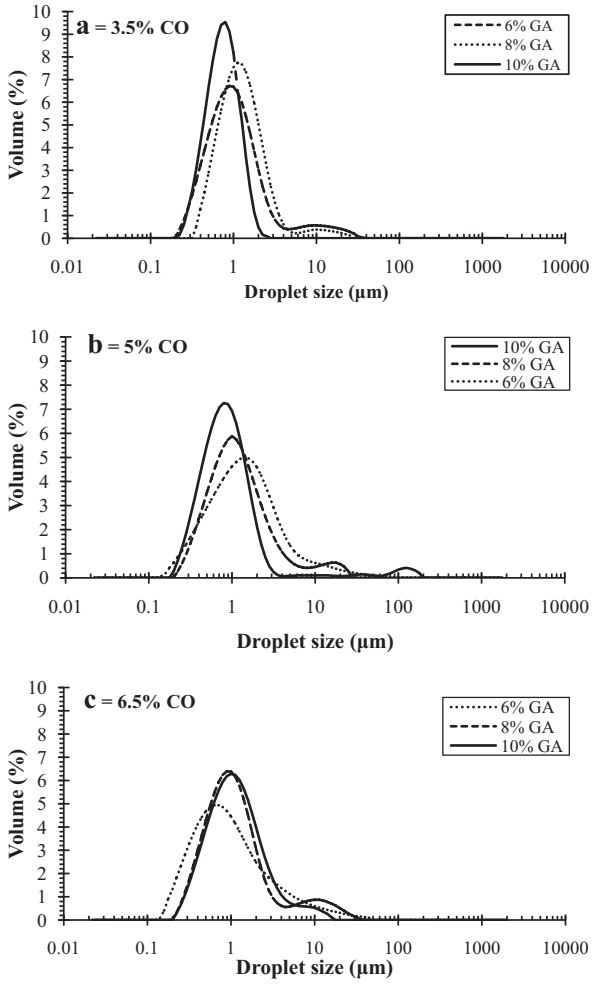

Fig. 3. Droplet size distribution of the emulsions containing bacterial CTX in the different concentrations of CO and GA for the same content of XG (=0.1%, w/w).

This may be explained by the fact that at a high GA concentration, the emulsion is relatively well covered by GA, inhibiting the droplet aggregation through steric and electrostatic repulsion and forming a smaller droplet along with narrow size distribution (Fig. 3a–c) (Huang et al., 2001; Mohagheghi, Rezaei, Labbafi, & Mousavi, 2011). Fig. 3a–c shows droplet size distribution of the prepared emulsions at different concentrations of GA and CO used with constant content of XG (0.10%, w/w). As considered in this figure, an increase of GA content in range and initial concentration of CO were associated with high minimum PDI and D_{32}. The optimum content of GA, XG and CO for the minimum PDI value ($Y_2 = 1.533$) was around 10% (w/w), 0.10% (w/w) and 3.50% (w/w), respectively.

3.4. Analysis of influence of variables on specific surface area (SSA) of droplets

As given in Table 3, it may be found that SSA (Y_3) was related to the linear effect of GA content and CO concentration ($p < 0.0001$). The quadratic terms of XG and CO concentrations were significant ($p < 0.001$, $p < 0.05$). The mutual interaction of XG content with CO concentration was also significant ($p < 0.0001$). The linear effect of GA showed the most significant ($p < 0.05$) effect on SSA (Table 2). Koocheki and Kadkhodaee (2011) also found that by increasing the emulsifier concentration, SSA increased in a parabolic manner. It is well known that decreased D_{32} results in increase in SSA of emulsion droplets (Tan & Misran, 2008). In fact, smaller droplets have a larger SSA and so more emulsifier is needed to surround

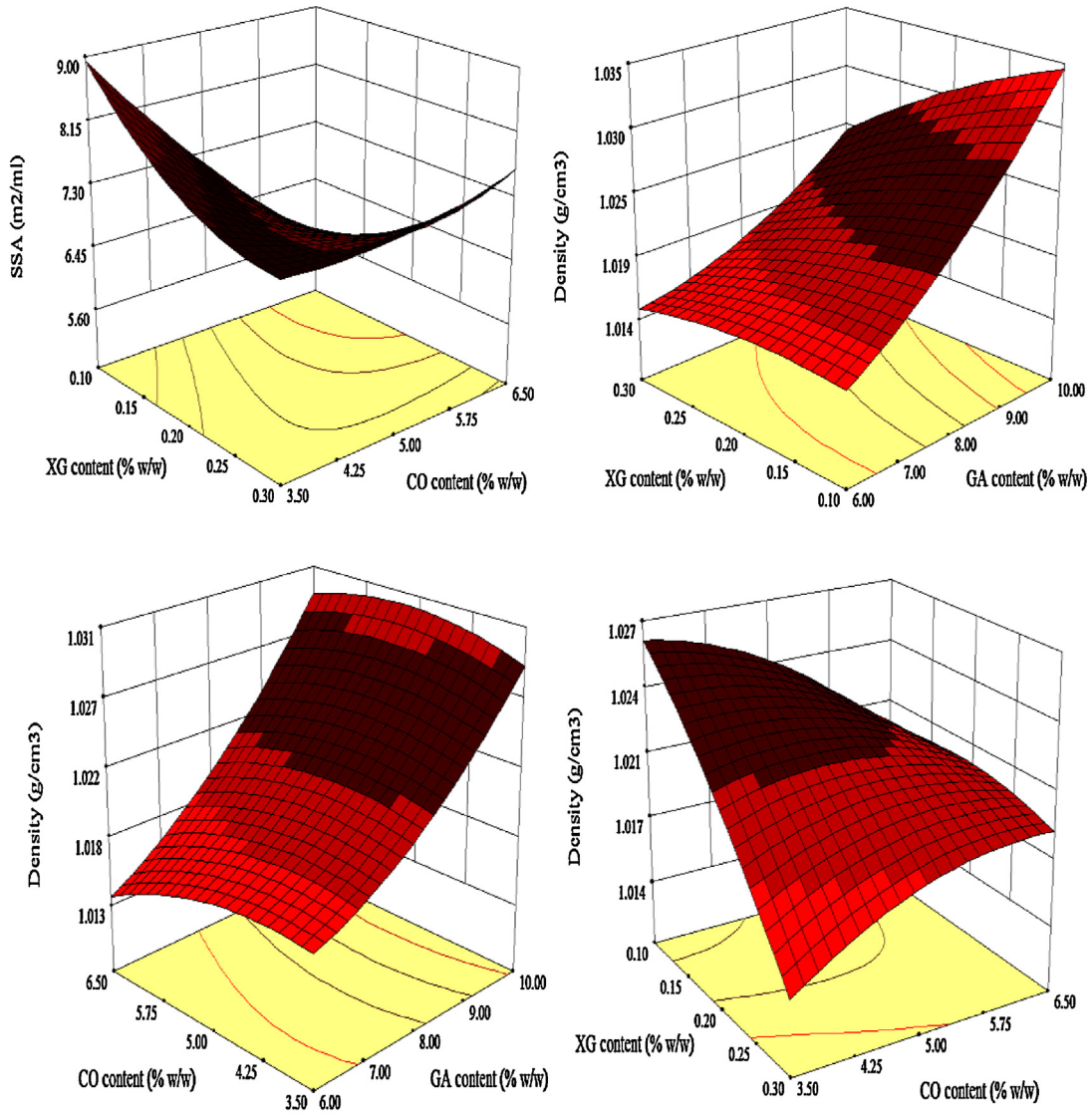

Fig. 4. 3D surface plots showing the significant ($p < 0.05$) interaction effects on the variation of SSA of droplets (a) and density (b–d) of the emulsions containing bacterial CTX.

the droplets, produce a stable system, and form a barrier against coalescence (Rousseau, 2000). Fig. 4a shows the effect of XG and CO variables on SSA value for a fixed level of GA in the emulsions. Increases in XG content resulted in increased SSA, although this property reduced sharply with increased CO concentration. Increasing the SSA at higher XG content is probably due to the increase in the continuous phase viscosity and the creation of a network, which prevents the oil droplets from coalescing (Huang et al., 2001; Koocheki & Kadkhodaee, 2011). The highest response for SSA in the ranges studied ($Y_3 = 10.00\ m^2/ml$) was observed when the emulsion was produced with 10% (w/w) GA, 0.18% (w/w) XG and 3.50% (w/w) CO.

3.5. Analysis of influence of variables on emulsion density

As revealed in Table 3, the density value (Y_4) was significantly influenced by the linear, quadratic and interaction effects of all independent variables studied ($p < 0.0001$, $p < 0.001$, $p < 0.01$, $p < 0.05$). The results showed that the linear effect of GA had the most significant ($p < 0.05$) effect on density character (Table 2). The 3D response surface graphs was plotted to better visualize the significant interaction effects of independent variables on the density (Fig. 4b–d). Fig. 4b and c shows that the density of CTX emulsions increased with increased proportions of GA. A possible reason is that increasing GA content would facilitate relatively smaller droplets adsorbing more GA at the interface of the oil droplets; this would increase the density of droplets and, consequently, decrease the creaming rate (Chanamai & McClements, 2000). However, the density amount of CO-in-water emulsion was negatively influenced by CO concentration (Fig. 4c and d). This fact may be explained by the negative effect of the oil phase on the density value (Mirhosseini, Tan, Hamid, & Yusof, 2008). These results were generally in agreement with those reported by Mirhosseini and Tan (2010) and Taherian et al. (2006). The individual optimum location led to the optimum density ($Y_4 = 1.0358\%$) for emulsion enriched with bacterial CTX was estimated to be achieved by a set level of 9.92%, 0.13% and 3.54% (w/w) for GA, XG and CO, respectively.

3.6. Optimal conditions and verification of the of models

The CTX emulsion would be considered an optimum product if the criteria used for graphical optimization led to (a) minimize D_{32} and PDI, (b) maximize SSA and (c) achieve the target value for density. The RSM package's response optimizer determined the

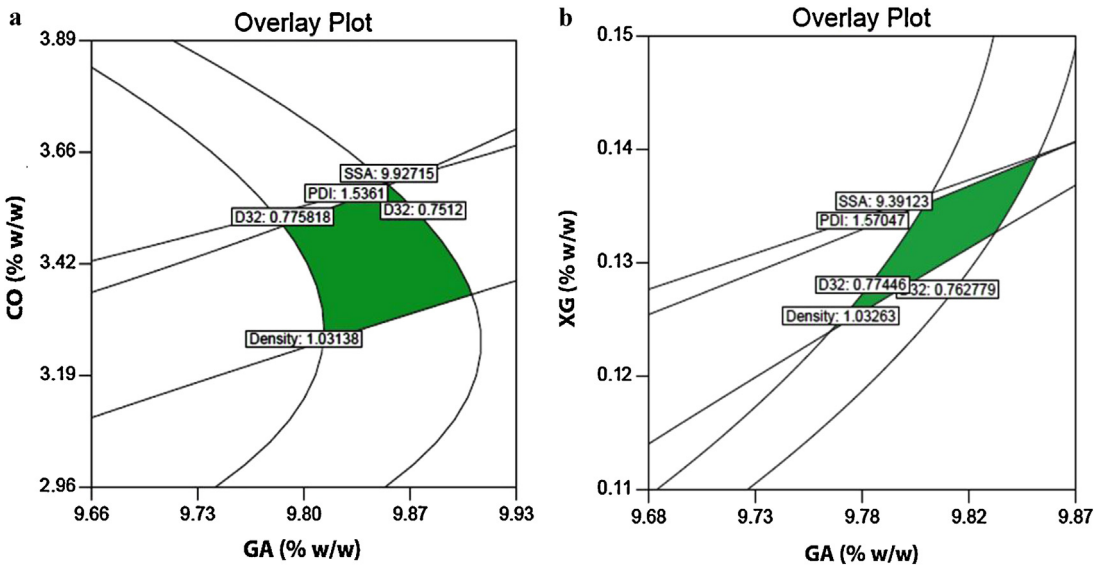

Fig. 5. The optimum region, obtained by overlaying contour plots of the four responses evaluated as a function of CO and GA (a, at constant XG content = 0.13%, w/w), and XG and GA (b, at constant CO concentration = 3.5%, w/w).

overall optimum region with high total desirability ($D = 0.888$) to be at 9.85% (w/w) GA, 0.13% (w/w) XG and 3.50% (w/w) CO. The corresponding predicted response values under the optimum conditions for D_{32}, PDI, SSA and density of the CTX emulsion were 752 μm, 1.533, 9.995 m^2/ml and 1.0357 g/cm^3, respectively. This set of conditions was determined to be optimum by the RSM optimization approach and was also applied to validate experimentally and predict the values of the responses by the models. For the graphical interpretation of independent variables interactions, the use of an overlay plot of the regression model has been highly recommended (Mason et al., 2003). The range of optimum conditions can be visualized by superimposing the contours for the various response surfaces in an overlay plot, which defines a region in which optimum values for all responses can be obtained. The yellow/shaded areas on the overlay plots Fig. 5a and b are the regions that meet the proposed criteria.

In order to validate the adequacy of the model equations, five runs of additional confirmation experiments were carried out under the optimal conditions. Under the suggested optimal conditions, the corresponding experimental values for D_{32}, PDI, SSA and density of the desirable CTX emulsion were 0.788 ± 0.054 μm, 1.665 ± 0.251, 9.849 ± 0.154 m^2/ml and 1.0342 ± 0.0006 g/cm^3, respectively. No significant ($p > 0.05$) difference was found between the actual values and predicted values. At this optimal formulation, the emulsion stability and the EE of CTX were 96.4% and 94.17%, respectively. Therefore, the presented models can be used to optimize the main components of the emulsions containing CTX biosynthesized by *D. natronolimnaea* HS-1.

4. Conclusion

Response surface methodology (RSM) was used to study the effects of three factors, i.e. GA, XG and CO concentrations on the droplet size and density characteristics of emulsions fortified with CTX produced by *D. natronolimnaea* HS-1 as a natural antioxidant were evaluated. Second-order polynomial models with high R^2 (0.970–0.995) values were developed to predict these properties as a function of the selected variables. The linear effect of GA, the quadratic effect of XG and the interaction effect of XG and CO were the most significant ($p < 0.05$) effects on all of the studied properties. According to the regression equations, the optimum conditions for experiment parameters were obtained with GA content of 9.85% (w/w), XG content of 0.13% (w/w) and CO concentration of 3.50% (w/w). A high stability and an ideal EE of CTX was observed at this optimum formulation. There is a very good agreement between the predicted results by CCRD and the measured ones obtained experimentally, indicating the high accuracy of the RSM.

Acknowledgements

The authors would like to extend their appreciation for the financial support provided by the University of Tehran and ZamZam Iran Co. for its technical and financial assistance.

References

Baş, D., & Boyaci, I. H. (2007). Modeling and optimization I: Usability of response surface methodology. *Journal of Food Engineering*, *78*, 836–845.
Batista, A. P., Raymundo, A., Sousa, I., & Empis, J. (2006). Rheological characterization of coloured oil-in-water food emulsions with lutein and phycocyanin added to the oil and aqueous phases. *Food Hydrocolloids*, *20*, 44–52.
Buffo, R. A., Reineccius, G. A., & Oehlert, G. W. (2001). Factors affecting the emulsifying and rheological properties of gum acacia in beverage emulsions. *Food Hydrocolloids*, *15*, 53–66.
Chanamai, R., & McClements, D. J. (2000). Impact of weighting agents and sucrose on gravitational separation of beverage emulsions. *Journal of Agricultural and Food Chemistry*, *48*, 5561–5565.
Cruz, A. G., Faria, J. A. F., Granato, D., Cavalcanti, R., & Walter, E. H. M. (2010). Processing optimization of probiotic yogurt containing glucose oxidase using response surface methodology. *Journal of Dairy Science*, *93*, 5059–5068.
Dickinson, E., Galazka, V. B., & Anderson, D. M. W. (1991). Emulsifying behaviour of gum arabic. Part 1: Effect of the nature of the oil phase on the emulsion droplet-size distribution. *Carbohydrate Polymers*, *14*, 373–383.
Dłuzewska, E., Stobiecka, A., & Maszewska, M. (2006). Effect of oil phase concentration on rheological properties and stability of beverage emulsions. *ACTA Scientiarum Polonorum Technologia Alimentaria*, *5*, 147–156.
Gharibzahedi, S. M. T., Mousavi, S. M., Hamedi, M., & Ghasemlou, M. (2012). Response surface modeling for optimization of formulation variables and physical stability assessment of walnut oil-in-water beverage emulsions. *Food Hydrocolloids*, *26*, 293–301.
Gharibzahedi, S. M. T., Mousavi, S. M., Hamedi, M., & Khodaiyan, F. (2013). Application of response surface modeling to optimize critical structural components of walnut–beverage emulsion with respect to analysis of the physicochemical aspects. *Food and Bioprocess Technology*, *6*(2), 456–469.
Gharibzahedi, S. M. T., Mousavi, S. M., Hamedi, M., Khodaiyan, F., & Razavi, S. H. (2012). Development of an optimal formulation for oxidative stability of walnut-beverage emulsions based on gum arabic and xanthan gum using response surface methodology. *Carbohydrate Polymers*, *87*, 1611–1619.
Gharibzahedi, S. M. T., Mousavi, S. M., Khodaiyan, F., & Hamedi, M. (2012). Optimization and characterization of walnut beverage emulsions in relation to their

composition and structure. *International Journal of Biological Macromolecules*, *50*, 376–384.
Gharibzahedi, S. M. T., Razavi, S. H., & Mousavi, S. M. (2012). Developing an emulsion model system containing canthaxanthin biosynthesized by *Dietzia natronolimnaea* HS-1. *International Journal of Biological Macromolecules*, *51*, 618–626.
Gharibzahedi, S. M. T., Razavi, S. H., & Mousavi, S. M. (2013). Psyllium husk gum: An attractive carbohydrate biopolymer for the production of stable canthaxanthin emulsions. *Carbohydrate Polymers*, *92*, 2002–2011.
Gharibzahedi, S. M. T., Razavi, S. H., Mousavi, S. M., & Moayedi, V. (2012). High efficiency canthaxanthin production by a novel mutant isolated from *Dietzia natronolimnaea* HS-1 using central composite design analysis. *Industrial Crops and Products*, *40*, 345–354.
Granato, D., Castro, I. A., Neves, L. S., & Masson, M. L. (2010). Physical stability assessment and sensory optimization of a dairy-free emulsion using response surface methodology. *Journal of Food Science*, *73*, 149–155.
Harnsilawat, T., Pongsawatmanit, R., & Mcclements, D. J. (2006). Stabilization of model beverage cloud emulsions using protein-polysaccharide electrostatic complexes formed at the oil-water interface. *Journal of Agricultural and Food Chemistry*, *54*, 5540–5547.
Higiro, J., Herald, T. J., & Alavi, S. (2006). Rheological study of xanthan and locust bean gum interaction in dilute solution. *Food Research International*, *39*, 165–175.
Hojjati, M., Razavi, S. H., Rezaei, K., & Gilani, K. (2011). Spray drying microencapsulation of natural canthaxantin using soluble soybean polysaccharide as a carrier. *Food Science and Biotechnology*, *20*(1), 63–69.
Huang, X., Kakuda, Y., & Cui, W. (2001). Hydrocolloids in emulsions: particle size distribution and interfacial activity. *Food Hydrocolloids*, *15*, 533–542.
Khodaiyan, F., Razavi, S. H., & Mousavi, S. M. (2008). Optimization of canthaxanthin production by *Dietzia natronolimnaea* HS-1 from cheese whey using statistical experimental methods. *Biochemical Engineering Journal*, *40*, 415–422.
Koocheki, A., & Kadkhodaee, R. (2011). Effect of *Alyssum homolocarpum* seed gum, Tween 80 and NaCl on droplets characteristics flow properties and physical stability of ultrasonically prepared corn oil-in-water emulsions. *Food Hydrocolloids*, *25*, 1149–1157.
Mason, R. L., Richard, F., Gunst, R. F., & Hess, J. L. (2003). *Statistical design and analysis of experiments with applications to engineering and science*. Hoboken, NJ: John Wiley & Sons, Inc.
Mirhosseini, H., Tan, C. P., Hamid, N. S. A., & Yusof, S. (2008). Optimization the contents of arabic gum, xanthan and orange oil affecting on turbidity, average particle size polydispersity index and density in orange beverage emulsion. *Food Hydrocolloids*, *22*, 1212–1223.
Mirhosseini, H., & Tan, C. P. J. (2010). Discrimination of orange beverage emulsions with different formulations using multivariate analysis. *Journal of the Science of Food and Agriculture*, *90*, 1308–1316.
Mohagheghi, M., Rezaei, K., Labbafi, M., & Mousavi, S. M. (2011). Pomegranate seed oil as a functional ingredient in beverages. *European Journal of Lipid Science and Technology*, *113*(6), 730–736.
Myers, R. H., & Montgomery, R. C. (2002). *Response surface methodology, process and product optimization using design experiment*. New York: John Wiley.
Nikiforidis, C. V., & Kiosseoglou, V. (2010). Physicochemical stability of maize germ oil body emulsions as influenced by oil body surface-xanthan gum interactions. *Journal of Agricultural and Food Chemistry*, *58*, 527–532.
Razavi, S. H., Blanchard, F., & Marc, I. (2006). UV–HPLC/APCI MS method for separation and identification of the carotenoids produced by *Sporobolomyces ruberrimus* H110. *Iranian Journal of Chemistry & Chemical Engineering*, *25*, 1–10.
Rousseau, D. (2000). Fat crystals and emulsion stability – a review. *Food Research International*, *33*, 3–14.
Taherian, A. R., Fustier, P., & Ramaswamy, H. S. (2006). Effect of added oil and modified starch on rheological properties, droplet size distribution opacity and stability of beverage cloud emulsions. *Journal of Food Engineering*, *77*, 687–696.
Tan, C. T. (1990). Beverage emulsion. In K. Larsson, & S. E. Friberg (Eds.), *Food emulsions* (pp. 445–478). New York, NY: Marcel Dekker.
Tan, H. W., & Misran, M. (2008). Stability of concentrated olive oil-in-water emulsion. *Chinese Journal of Chemistry*, *26*, 1963–1968.
Yue, P. F., Lu, X. Y., Zhang, Z. Z., Yuan, H. L., Zhu, W. F., Zheng, Q., et al. (2009). The study on the entrapment efficiency and in vitro release of puerarin submicron emulsion. *AAPS PharmSciTech*, *10*(2), 376–383.